JOURNAL OF SOLID STATE CHEMISTRY 95, 126–135 (1991)

The Mixed Orthoborate Pyroborates $Sr_2Sc_2B_4O_{11}$ and $Ba_2Sc_2B_4O_{11}$: Pyroborate Geometry

PAUL D. THOMPSON, JINFAN HUANG, ROBERT W. SMITH, AND DOUGLAS A. KESZLER*

Center for Advanced Materials Research and Department of Chemistry, Oregon State University, Gilbert Hall 153, Corvallis, Oregon 97331-4003

Received December 26, 1990; in revised form June 26, 1991

Two new alkaline-earth scandium borates, the mixed orthoborate pyroborates $A_2Sc_2B_4O_{11}$ (A = Sr or Ba), have been synthesized and structurally characterized by single-crystal X-ray diffraction methods. The compounds may be represented by the descriptive formula $A_2Sc_2(BO_3)_2(B_2O_5)$ which indicates two orthoborate groups and one pyroborate group for each formula unit. The Sr compound crystallizes in the triclinic system in space group $P\bar{1}$ (No. 2) with cell parameters a = 6.293(3), b = 7.285(3), c = 5.084(3) Å, α = 90.71(5), β = 104.68(4), γ = 78.07(4)°, and V = 220.4(4) Å^3. The structure exhibits layers composed of an admixture of orthoborate and pyroborate groups. These layers are interleaved by Sr atoms occupying 8-coordinate sites and Sc atoms occupying distorted octahedral sites. The geometry of the pyroborate group is unusual, exhibiting the angle B–O–B = 180°. The Ba compound crystallizes in the monoclinic system in space group $C2/c$ (No. 15) with cell parameters a = 16.022(2), b = 9.354(2), c = 6.343(2) Å, β = 100.42(2)°, and V = 934.8(7) Å^3. The structure contains two types of Sc-centered, distorted octahedral sites. One type is isolated by bridging borate groups while members of the second type condense along *trans* edges to form one-dimensional chains. The chains are bridged by Ba atoms, simple orthoborate groups, and a unique pyroborate group. The principal planes of the pyroborate are rotated by 76.8°, one relative to the other, and the angle B–O–B = 112.1(7)°. Results of extended Hückel calculations indicate facile rotation of the principal planes of the pyroborate group is expected.

Introduction

The simplest condensation of triangular groups in borate chemistry affords the pyroborate anion $B_2O_5^{4-}$ Scheme 1. In reported examples of pyroborates (*1–14*), the terminal BO_2 planes pivot about the torsion angles τ_1 and τ_2 to afford deviations from coplanarity that range from 1.6 to 67.0° while the central B–O–B angle ranges from 111.8 to 138.7°. In this paper we describe two new, mixed orthoborate pyroborates $Sr_2Sc_2B_4O_{11}$ and $Ba_2Sc_2B_4O_{11}$ in which the pyroborate groups adopt geometries with new maxima for the deviation from planarity and the B–O–B angle. A simple analysis of the bonding in the group is also presented.

The compound $Sr_2Sc_2B_4O_{11}$ has resulted from our continuing interest in phase equilibria in the system $SrO–Sc_2O_3–B_2O_3$ (*15*). The compound $Ba_2Sc_2B_4O_{11}$ is one of three new materials resulting from our examination of the system $BaO–Sc_2O_3–B_2O_3$.

* To whom correspondence should be addressed.

0022-4596/91 $3.00

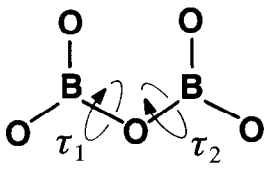

SCHEME 1

Preparation and X-Ray Work

Powdered samples of the material $Sr_2Sc_2B_4O_{11}$ were prepared by separately heating the stoichiometric mixtures $Sr_2B_2O_5$ + $2ScBO_3$ and $\frac{2}{3}Sr_3B_2O_6$ + $2ScBO_3$ + $\frac{1}{3}B_2O_3$. The binary borates were prepared by heating stoichiometric quantities of the reagents $Sr(NO_3)_2$ (reagent grade, J. T. Baker), Sc_2O_3 (reagent grade, Boulder Scientific), and B_2O_3 (99.99%, Alfa) at 950°C for 12 hr. Combinations of the binary borates were pressed into pellets and annealed in Pt crucibles at 950°C for 12 hr and 1050°C for 12 hr. The X-ray powder diffraction pattern of each sample compares well to the pattern calculated by using the program LAZY-PULVERIX (*16*) and the results of the structure determination.

Single crystals of the compound were isolated from a mixture containing the phases $Sr_3B_2O_6$ and $ScBO_3$ in the molar ratio 1 : 4 that was melted at 1465°C and cooled to room temperature by simply turning the power to the furnace off. A crystal of dimensions 0.1 × 0.2 × 0.25 mm was physically separated from the matrix and mounted on a Rigaku AFC6R diffractometer for data collection. Unit cell parameters were established by least-squares analysis of 24 reflections in the range $30.1 \leq 2\theta \leq 34.1°$; crystal data are listed in Table I. Data were collected by using the ω-2θ scan method with a scan speed of 32°/min in 2θ to sin $\theta_{max}/\lambda = 0.648$ Å^{-1}. From 1125 reflections measured in the range of indices $-7 \leq h \leq 7$, $-9 \leq k \leq 9$, and $0 \leq l \leq 6$, a total of 970 data were observed ($F_o^2 > 3\sigma(F_o^2)$). The structure was solved and refined with programs from the TEXSAN crystallographic software package (*17*). Patterson methods afforded the location of the Sr and Sc atoms. The positions of the remaining atoms were subsequently found by analysis of difference electron density maps. Following refinement of the model with isotropic thermal parameters on each atom, the data were corrected for absorption with the computer program DIFABS (*18*). Final least-squares refinement on $|F|$ with anisotropic thermal parameters on each atom resulted in the final residuals $R = 0.024$ and $R_w = 0.034$ with $\Delta/\sigma = 0.002$. The final difference electron density map afforded a maximum peak = 0.962 e/Å^3, corresponding to 2.5% of a Sr atom. Final positional and thermal parameters are listed in Table II.

The compound $Ba_2Sc_2B_4O_{11}$ was initially observed during an examination of the phase line $Ba_2B_2O_5$–$ScBO_3$. A powdered sample of the material was prepared by grinding a stoichiometric mixture of the reagents $Ba(NO_3)_2$ (AR Grade, Mallinkrodt), Sc_2O_3 (99.9%, Aesar), and B_2O_3 (99.9%, Alfa) followed by heating in a Pt crucible at 700°C for 12 hr, 900°C for 3 hr, and 1000°C for 20 min. The powder X-ray diffraction

TABLE I

CRYSTALLOGRAPHIC DATA

Formula	$Sr_2Sc_2B_4O_{11}$	$Ba_2Sc_2B_4O_{11}$
Formula weight (amu)	484.39	583.81
a (Å)	6.293(3)	16.022(2)
b (Å)	7.285(3)	9.354(2)
c (Å)	5.084(3)	6.342(2)
α (°)	90.71(5)	90
β (°)	100.68(4)	100.42(2)
γ (°)	78.07(4)	90
V (Å^3)	220.4(4)	934.8(7)
Z	1	4
Space group	$P\bar{1}$ (No. 2)	C2/c (No. 15)
T (K)	296	296
λ	0.71069 Å, Mo$K\alpha$ (graphite monochromated)	
D_{calc} (g cm^{-3})	3.65	4.15
μ (cm^{-1})	132.11	97.66
Transmission coefficients	0.775–1.333	0.930–1.091
R (F_o)	0.024	0.021
R_w (F_o)	0.034	0.024

TABLE II

POSITIONAL PARAMETERS AND EQUIVALENT ISOTROPIC THERMAL PARAMETERS FOR $Sr_2Sc_2B_4O_{11}$

	x	y	z	B_{eq}
Sr	0.19241(5)	0.16409(4)	0.77598(6)	0.64(2)
Sc	0.2833(1)	0.64716(9)	0.8147(1)	0.45(3)
B1	0.6569(7)	0.1017(5)	0.6456(8)	0.6(2)
B2	0.2188(6)	0.3918(5)	0.2785(8)	0.6(1)
O1	0.7933(4)	0.1517(4)	0.5066(5)	0.8(1)
O2	0.0524(4)	0.2952(4)	0.1764(5)	0.9(1)
O3	0.6598(5)	0.1331(4)	0.9081(5)	0.9(1)
O4	0.2567(5)	0.4440(4)	0.5381(5)	0.9(1)
O5	0.3564(4)	0.4419(3)	0.1101(5)	0.7(1)
O6	$\frac{1}{2}$	0	$\frac{1}{2}$	1.8(2)

pattern of the sample compares well to that calculated from the results of the single-crystal structure determination.

Single crystals were isolated from a melt having the composition $BaO:Sc_2O_3:B_2O_3 = 6:3:5$ that was cooled from 1250 to 950°C at 2°C/hr then 80°C/hr to room temperature. A crystal of dimensions 0.15 × 0.15 × 0.10 mm was mounted for data collection. Unit-cell parameters were derived from a least-squares analysis of 21 reflections in the range $30 \leq 2\theta \leq 40°$ that were automatically centered on the same diffractometer. Intensity data were collected covering the range of indices $0 \leq h \leq 19$, $0 \leq k \leq 11$, and $-8 \leq l \leq 8$ with the ω-2θ scan technique at a scan speed of 32°/min in 2θ and a scan width $\Delta\omega = (1.47 + 0.3 \tan\theta)°$. The intensities of three standard reflections, measured after each block of 150 data, exhibited excursions of less than 1.6%. From 945 reflections measured to $2\theta = 50°$, 716 unique data having $F_o^2 > 3\sigma(F_o^2)$ were obtained.

The positions of the atoms Ba and Sc1 were ascertained from the results of the direct methods program MITHRIL (*19*); the remaining atomic positions were determined by subsequent analyses of difference electron density maps. Following refinement of isotropic thermal parameters the data were corrected for absorption with the computer program DIFABS. Final refinement on $|F|$ with those data having $F_o^2 > 3\sigma(F_o^2)$, 81 variables, and 716 observations resulted in the final residuals $R = 0.021$ and $R_w = 0.024$. The largest peak in the final difference electron density map corresponds to 0.99% of a Ba atom. Final atomic parameters are given in Table III.

Structures

A labeled drawing of the contents of the unit cell of the compound $Sr_2Sc_2B_4O_{11}$ is shown in Fig. 1, and a perspective view along the c axis is shown in Fig. 2. The structure is built from mixed orthoborate, pyroborate layers, Scheme 2, stacking approximately along the direction $[1\bar{1}0]$; Sr and Sc atoms are interleaved between successive layers. The Sr atom occupies an 8-coordinate site resembling a distorted cube. The Sc atom occupies a distorted octahedron; two of these octahedra share an edge (O5 · · · O5) across the borate layer to form a bioctahedral dimer (Fig. 2). These dimers are separated and isolated along the c axis by intervening borate groups.

TABLE III

POSITIONAL PARAMETERS AND EQUIVALENT ISOTROPIC THERMAL PARAMETERS FOR $Ba_2Sc_2B_4O_{11}$

	x	y	z	B_{eq}
Ba	0.36227(3)	0.16484(6)	0.07436(8)	0.56(2)
Sc1	$\frac{1}{4}$	$\frac{1}{4}$	$\frac{1}{2}$	0.33(8)
Sc2	0	0	0	0.33(8)
B1	0.3297(6)	0.499(1)	0.247(2)	0.4(1)
B2	0.4479(6)	0.169(1)	0.587(1)	0.5(1)
O1	0.4127(4)	0.4854(7)	0.2044(9)	0.6(2)
O2	0.2165(4)	0.1209(6)	−0.263(1)	0.7(2)
O3	0.3673(4)	0.1313(7)	−0.478(1)	0.8(2)
O4	0.2020(4)	0.1307(6)	0.233(1)	0.6(2)
O5	0.4898(4)	0.2757(6)	0.501(1)	0.9(2)
O6	$\frac{1}{2}$	0.82(1)	$\frac{3}{4}$	1.2(2)

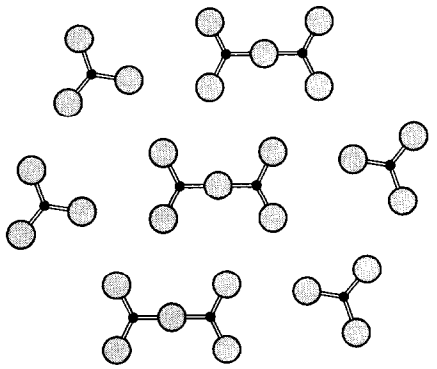

SCHEME 2

Selected interatomic distances and angles are listed in Table IV. Sr–O distances range from 2.519(3) to 2.807(3) Å with an average length of 2.64(11) Å that compares to the value 2.63 Å computed from crystal radii (*20*). The Sc–O distances in the distorted octahedron range from 2.032(3) to 2.152(3) Å with an average distance of 2.11(5) Å that compares to the value 2.125 Å computed from crystal radii. The angles O5–Sc–O5, 88.1(1)°, and O1–Sc–O5, 99.3(1)°, demonstrate the extent of the distortion from an ideal octahedral geometry.

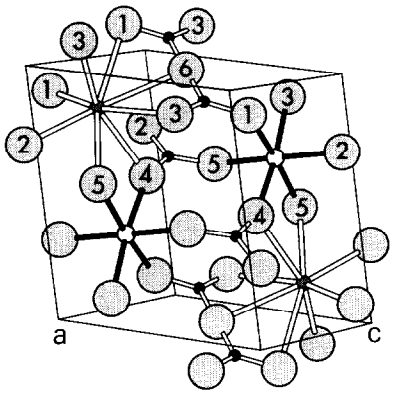

FIG. 1. Labeled sketch of the contents of a unit cell of the compound $Sr_2Sc_2B_4O_{11}$. The small shaded circles represent *A* atoms (*A* = Sr or Ba), the open circles represent Sc atoms, the small filled circles represent B atoms, and the large shaded circles represent *O* atoms, here, and in ensuing figures.

TABLE IV

SELECTED BOND DISTANCES (Å) AND ANGLES (°) FOR $Sr_2Sc_2B_4O_{11}$

Sr–O1	2.695(3)	O1–Sr–O6	50.79(6)
Sr–O1	2.557(3)	O3–Sr–O6	50.23(6)
Sr–O2	2.519(3)	O1–Sr–O3	93.89(8)
Sr–O3	2.807(3)	O1–Sr–O2	138.14(8)
Sr–O3	2.574(3)	O3–Sr–O5	63.37(8)
Sr–O4	2.536(3)	O3–Sr–O5	100.5(1)
Sr–O5	2.693(3)	O1–Sr–O1	71.2(1)
Sr–O6	2.743(1)	O5–Sr–O6	115.05(9)
Sc–O1	2.101(3)	O1–Sc–O2	89.8(1)
Sc–O2	2.079(3)	O1–Sc–O5	173.9(1)
Sc–O3	2.145(3)	O1–Sc–O5	99.3(1)
Sc–O4	2.032(3)	O2–Sc–O5	90.6(1)
Sc–O5	2.145(3)	O2–Sc–O4	96.0(1)
Sc–O5	2.152(3)	O2–Sc–O5	168.8(1)
B1–O1	1.346(5)	O1–B1–O3	127.1(3)
B1–O3	1.348(5)	O1–B1–O6	115.6(3)
B1–O6	1.411(4)	O3–B1–O6	117.3(3)
B2–O2	1.346(5)	O1–B1–O3	127.1(3)
B2–O4	1.345(5)	O2–B2–O5	117.7(3)
B2–O5	1.406(4)	O4–B2–O5	122.1(3)

The triangular orthoborate group is normal with B–O distances ranging from 1.345(5) to 1.406(4) Å, and the largest angular distortion is exhibited by O2–B2–O4, 117.7(3)°. The pyroborate group, however, adopts an unusual geometry, exhibiting a planar orientation with a B–O–B angle of 180° and the central O atom occupying a site with inversion symmetry. The B1–O6 distance involving the central O atom is longer than the B–O distances involving the terminal O atoms. The magnitude of the thermal parameter for the central O6 atom is consistent with the long nonbonded O6 · · · O distances. The O6 · · · O1 and O6 · · · O3 distances, 2.332(3) and 2.356(3) Å, respectively, of the terminal BO_2 groups are comparable to the average O · · · O distance, 2.37(3) Å, within each BO_3 triangle. Outside the triangle the shortest O6 · · · O distance is 3.240(3) Å (O6 · · · O2), which contrasts

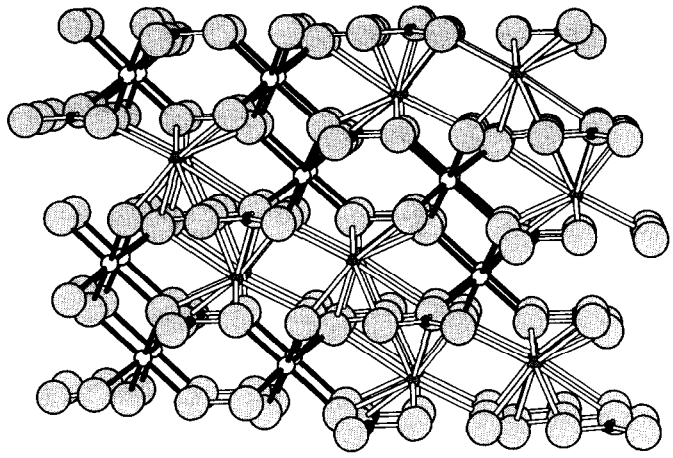

FIG. 2. Perspective view of the structure of $Sr_2Sc_2B_4O_{11}$ along the c axis.

to the other O atoms which have five O · · · O interactions in the range 2.891(4) to 3.241(4) Å. With contacts to two Sr atoms and two B atoms the central atom O6 exhibits a distorted square-planar coordination; atoms O2 and O4 bind three cations, and the remaining O atoms are bound by four cations in distorted tetrahedral arrangements. By using the coordination geometries described above and the bond-valence method (*21*), we have found the valences of all atoms to be within 4% of their characteristic integral values.

Selected interatomic distances and angles for the compound $Ba_2Sc_2B_4O_{11}$ are listed in Table V. A labeled projection of the contents of the unit cell is shown in Fig. 3. Diagrams of the scandium borate matrix are shown in Fig. 4. Two inequivalent Sc atoms are present in the structure, each occupying a distorted octahedral site. Chains of Sc1-centered octahedra sharing edge O6 · · · O6 extend parallel to the c axis with pairs of these octahedra linked through the vertices of the bridging pyroborate group (Fig. 4). The O atoms of the shared octahedral edges are also vertices of the BO_3 groups which stack one upon the other along the c axis. The octahedron occupied by atom Sc2 is isolated from the octahedra occupied by atom Sc1 and other octahedra of the same type by the intervening orthoborate and pyroborate groups. The Ba atom occupies a large hollow in the matrix, connecting to

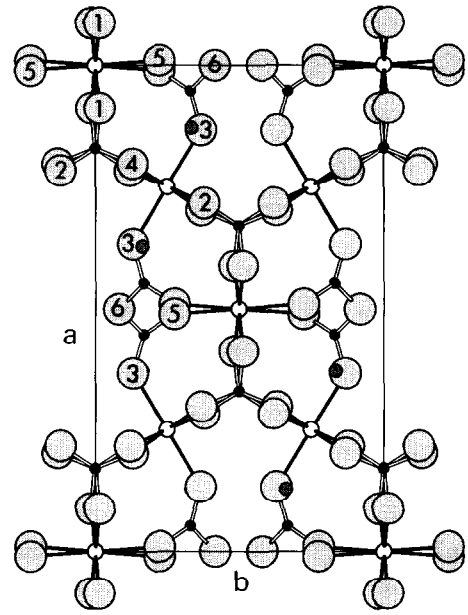

FIG. 3. Labeled projection of the structure of $Ba_2Sc_2B_4O_{11}$.

TABLE V
SELECTED BOND DISTANCES (Å) AND ANGLES (°) FOR $Ba_2Sc_2B_4O_{11}$

Ba–O5	2.706(4)	O2–Ba–O4	55.5(1)
Ba–O2	2.752(4)	O2–Ba–O4	70.5(1)
Ba–O4	2.784(4)	O3–Ba–O4	94.4(1)
Ba–O3	2.797(4)	O4–Ba–O4	94.4(1)
Ba–O3	2.845(5)	O5–Ba–O3	110.6(1)
Ba–O2	2.902(4)	O2–Ba–O3	142.9(1)
Ba–O4	2.939(6)	O5–Ba–O4	161.7(1)
Ba–O1	3.173(5)		
Ba–O5	3.253(5)		
Ba–O6	3.365(5)		
Sc1–O4 ×2	2.060(4)	O4–Sc1–O3	88.2(2)
Sc1–O2 ×2	2.068(4)	O4–Sc1–O2	79.9(2)
Sc1–O3 ×2	2.164(4)		
Sc2–O1 ×2	2.077(4)	O1–Sc2–O5	89.8(2)
Sc2–O5 ×2	2.110(4)	O1–Sc2–O5	81.7(2)
Sc2–O1 ×2	2.129(4)		
B1–O1	1.411(8)	O1–B1–O2	118.7(6)
B1–O2	1.361(8)	O1–B1–O4	119.1(6)
B1–O4	1.350(8)	O2–B1–O4	122.2(6)
B2–O3	1.345(8)	O3–B2–O5	125.1(6)
B2–O5	1.361(8)	O3–B2–O6	118.4(6)
B2–O6	1.434(8)	O5–B2–O6	116.3(5)

eleven O atoms at distances ranging from 2.706(5) to 3.365(5) Å.

The unusual feature of the structure is the geometry adopted by the pyroborate group. The B2–O6–B2 angle is 112.1(7)° and the terminal BO_2 planes are slanted by 76.8°, Scheme 3. The conformation of the group affords three different O coordination modes, atom O3, 4-coordinate; atom O5, [3 + 1]-coordinate; and atom O6, [2 + 2]-coordinate, two normal distances to atom B2, and two long distances to Ba (Table V). We compute valences for the atoms from the bond-valence method as follows: Ba, 2.06; Sc1, 3.21; Sc2, 3.12; B1, 2.86; and B2, 2.90.

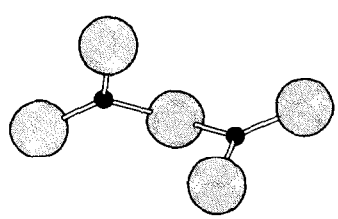

SCHEME 3

Infrared Measurements

Infrared spectra for the phases $Ba_2Sc_2B_4O_{11}$, $Sr_2Sc_2B_4O_{11}$, and $ScBO_3$ are shown in Fig. 5. Powdered samples were examined as dispersions (2 wt%) in KBr pellets by using a Starlab Sirius 100 FTIR spectrometer (Mattson Instruments Inc.). The spectrum of $ScBO_3$ exhibits three symmetry-allowed bands with contributions from two B isotopes present in their natural abundance ($^{10}B/^{11}B$ = 18/82). These bands are the out-of-plane bending modes (ω_2) occurring at 763 and 740 cm^{-1}, the doubly degenerate antisymmetric stretch (ω_3) at 1265 and 1234 cm^{-1}, and the degenerate in-plane mode at 639 cm^{-1}. These values correspond to those reported in the literature (*22*). Because the planar BO_3 group has D_3 symmetry in $ScBO_3$, the symmetric stretching mode (ω_1) is IR inactive whereas the BO_3 groups in the pyroborates have no imposed symmetry, making the modes active. This vibration has been observed near 950 cm^{-1} in other orthoborates, and is likely present in the spectra of the title compounds. The remaining peaks in the spectra of the Sr and Ba compounds arise from the fundamental modes of absorption of the pyroborate group. Assignment of the modes requires analyses of isotopically substituted samples; the data are presented here primarily for identification purposes.

Pyroborate Geometry

A broad distribution of B–O–B angles and torsion angles, τ_1 and τ_2, of the terminal BO_2 groups, Scheme 1, has been observed for the pyroborate group; B–O–B and interplanar angles for all structurally characterized examples are listed in Table VI. The B–O–B angle is observed to vary from 125 to 180° while a nearly planar arrangement

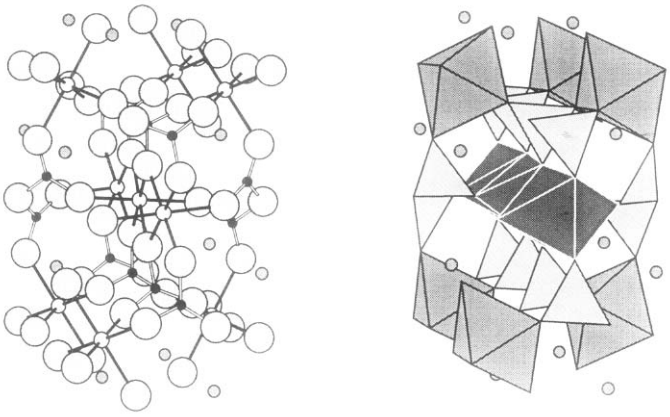

FIG. 4. Sketches of the structure of $Ba_2Sc_2B_4O_{11}$. Atom Sc1 occupies the darkest polyhedron in the sketch at right.

is maintained. We have examined selected conformations of the $B_2O_5^{4-}$ group by the extended Hückel method (*23*). Calculations were performed on planar geometries with B–O–B angles = 110, 120, 140, 160, and 180°. In each calculation all B–O distances were fixed at 1.37 Å. The most stable geometry in this series corresponds to B–O–B = 180° with a total energy = −787.9 eV. As the angle approaches 120° the magnitude of the total energy decreases only slightly. Be-

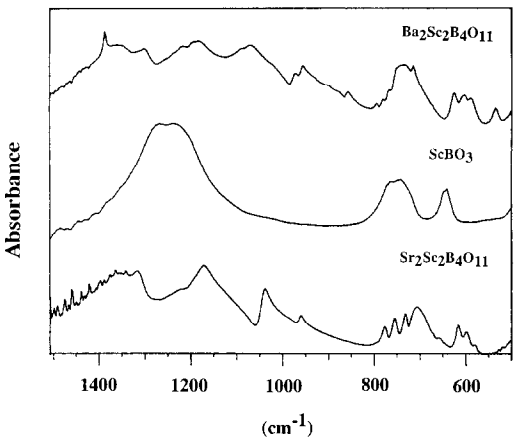

FIG. 5. Infrared absorption spectra for selected borates.

TABLE VI

B–O–B AND INTERPLANAR ANGLES FOR PYROBORATES

Compound	Space group	B–O–B angle	Interplanar angle	Ref.
$Sr_2Sc_2B_4O_{11}$	$P\bar{1}$	180°	0°	This work
$Sr_2ScLiB_4O_{10}$	$P2_1/n$	129.2°	1.6°	(*1*)
$Sr_2B_2O_5$	$P2_1/a$	140°	4.0°	(*2*)
$Sr_2ScLiB_4O_{10}$	$P2_1/n$	133.8°	8.9°	(*1*)
$Tl(NbO)B_2O_5$	$Pna2_1$	125.6°	10.6°	(*3*)
$Rb(NbO)B_2O_5$	Pn	116.5°	11.1°	(*4*)
$Rb(NbO)B_2O_5$	Pn	120.5°	11.8°	(*4*)
$Rb(NbO)B_2O_5$	Pn	127.0°	15.4°	(*4*)
$Rb(NbO)B_2O_5$	Pn	126.9°	15.7°	(*4*)
$Mg_2B_2O_5$	$P\bar{1}$	133.9°	16.1°	(*5*)
$Rb(NbO)B_2O_5$	Pn	127.7°	16.4°	(*4*)
$Co_2B_2O_5$	$P\bar{1}$	138.7°	18.8°	(*6*)
$Mg_2B_2O_5$	$P2_1/a$	138.0°	22.3°	(*7*)
$CaMgB_2O_5$	$Pca2_1$	123.3°	32.3°	(*8*)
$CaMgB_2O_5$	$P2_1/b$	122.0°	33.6°	(*9*)
$CaMgB_2O_5$	$Pca2_1$	124.1°	36.1°	(*8*)
$CaMnB_2O_5$	$P2_1/b$	120.1°	36.5°	(*10*)
$CaMgB_2O_5$	$Pca2_1$	115.6°	53.7°	(*8*)
$CaMgB_2O_5$	$Pca2_1$	118.1°	54.0°	(*8*)
$CaMgB_2O_5$	$P2_1/b$	119.5°	54.8°	(*9*)
$CaMgB_2O_5$	$Pca2_1$	113.4°	55.0°	(*8*)
$CaMgB_2O_5$	$Pca2_1$	118.0°	56.5°	(*8*)
$CaMnB_2O_5$	$P2_1/b$	111.8°	56.8°	(*10*)
$Na_4B_2O_5$	$C2/c$	120.2°	67.0°	(*11*)
$Ba_2Sc_2B_4O_{11}$	$C2/c$	112.1°	76.8°	This work

low 120°, a steep rise in the total energy occurs from increased O · · · O repulsive interactions. These repulsive interactions can be relieved by torsional motions about τ_1 and τ_2 which produce nonzero interplanar angles between the two terminal BO_2 groups. The total energy for a planar unit with B–O–B = 110° is −786.3 eV compared with the energy −787.0 eV of a group with the same B–O–B angle and an interplanar angle of 45°. The difference in energy arises from the repulsive interactions of the O lone pairs among the higher occupied orbitals. The smaller B–O–B angles are predominantly associated with the larger interplanar angles (Table VI). In silicates, as the Si–O–Si angle widens, the bridging Si–O interatomic distances shorten by a small amount (*24, 25*). A similar trend in the experimental data on pyroborates is not observed, although such a trend would be anticipated from our Hückel results. Overlap populations for the B–O bonds in the planar arrangement range from $B–O_{bridge}$, 0.61, and $B–O_{terminal}$, 0.67, for B–O–B = 110° to $B–O_{bridge}$, 0.66, and $B–O_{terminal}$, 0.65, for B–O–B = 180°. For larger B–O–B angles, a greater overlap between B(p)–O(p) orbitals increases the population that is commonly associated with a shorter bond length. Of course, this treatment neglects the nature and interactions of additional cations associated with the bridging O atom.

Values in Table VI also indicate a relatively smooth variation of interplanar angle from 0° to 76.8°. From consideration of charge distributions in simple electron-dot diagrams, the extent of π-electron delocalization through the central O atom is expected to be small because of the formal positive charge on this atom in one of the hybrids. With little π-electron density delocalized through the central O atom, no significant barriers to rotations about τ_1 or τ_2 are anticipated. This expectation is borne out by the results of calculations on geometries produced by incremental changes in τ_1 and τ_2 of 10° where no significant energetic differences were noted among the various geometries. These results are consistent with those listed in Table VI as well as the molecular structure of the isoelectronic species N_2O_5 (*26*) which has been modeled as a dynamic rotor with τ_1 and $\tau_2 \approx 30°$. Hence, in solids where the coordination and bonding requirements of all atoms must be simultaneously satisfied, a variety of geometries for the pyroborate group are observed.

Significance of Pyroborate Geometry

The geometry of the pyroborate group is important and relevant to the continued development of borates similar to LiB_3O_5 (LBO) (*27*) as nonlinear optical materials. The frequency converter LBO exhibits a threshold for second harmonic generation that is 100 times smaller than that of KDP (potassium dihydrogen phosphate) with an optical damage threshold near 25 GW/cm^2 with a 100-psec laser pulse. The polyborate anion in the structure has commonly been described as a fusion of B_3O_7 rings built from two B atoms in triangular coordination and one in tetrahedral coordination. An alternative description that emphasizes the principal chromophore in the structure is to consider the material to be a pyroborate with the pyroborate groups linked by tetrahedrally coordinated B atoms, Scheme 4. Because the pyroborate groups do not pack in distinct layers as in the materials $Sr_2Sc_2B_4O_{11}$, BaB_2O_4, and many other borates, the magnitude of the birefringence is relatively small. This feature coupled with a suitable constructive summation of microscopic hyperpolarizability coefficients affords a useful material with characteristics of small threshold for conversion and relative angular insensitivity to phasematching.

The largest microscopic hyperpolarizability coefficients associated with LBO derive from the pyroborate section of the borate matrix. These groups are not optimally

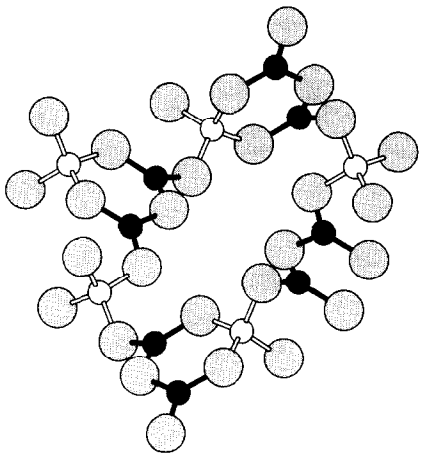

SCHEME 4

aligned in the material to afford the highest possible nonlinearity. Hence, the synthesis of new *acentric* pyroborates could well afford a nonlinearity higher than that of LBO. Higher nonlinearities should be observed in those materials crystallizing in layered structures having nearly planar groups identically oriented. These materials should also be highly birefringent, exhibiting many of the characteristics of the converter BaB_2O_4 (*28, 29*). The layered nature of a pyroborate structure can be disrupted by the coordination requirements of the associated cations as in the case of LBO or by the changeable nature of the interplanar angle. Where intermediate angles are encountered (~30–60°) in acentric samples, layered-type packings should be unfavored, and lower birefringence should be observed, likely with an intermediate nonlinearity.

Acknowledgments

This work was funded by the U.S. National Science Foundation, Solid State Chemistry Program. J.H. was supported under Subcontract B07620 administered by Lawrence Livermore National Laboratory. D.A.K. is grateful to the Alfred P. Sloan Foundation for a fellowship, 1989–1991.

References

1. P. D. THOMPSON AND D. A. KESZLER, *Solid State Ionics* **32/33,** 521 (1989).
2. H. BARTL AND W. SCHUCKMANN, *Neues Jahrb. Min. Monatsh.* **8,** 253 (1966).
3. M. GASPERIN, *Acta Crystallogr. Sect. B* **30,** 1181 (1974).
4. P. A. BAUCHER, M. GASPERIN, AND B. CERVELLE, *Acta Crystallogr. Sect. B* **32,** 2211 (1976).
5. S. BLOCK, G. BURLEY, A. PERLOFF, AND R. D. MASON, *J. Res. Natl. Bur. Stand.* **62,** 95 (1959).
6. S. BERGER, *Acta Chem. Scand.* **4,** 1054 (1950).
7. Y. TAKÉUCHI, *Acta Crystallogr.* **5,** 574 (1952).
8. O. V. YAKUBOVICH, M. A. SIMONOV, E. L. BELOKONEVA, YU. K. EGOROV-TISMENKO, AND N. V. BELOV, *Dokl. Acad. Nauk SSSR* **230,** 837 (1976).
9. O. V. YAKUBOVICH, N. A. YAMNOVA, B. M. SHCHEDRIN, M. A. SIMONOV, AND N. V. BELOV, *Dokl. Akad. Nauk SSSR* **228,** 842 (1976).
10. O. V. YAKUBOVICH, M. A. SIMONOV, AND N. V. BELOV, *Dokl. Akad. Nauk SSSR* **238,** 98 (1978).
11. H. KÖNIG, R. HOPPE, AND M. JANSEN, *Z. Anorg. Allg. Chem.* **449,** 91 (1979).
12. K. MACHIDA, G. ADACHI, AND J. SHIOKAWA, *Acta Crystallogr. Sect. B* **35,** 145 (1979).
13. YU. N. IL'IN, V. V. KRAVCHENKO, AND K. I. PETROV, *Russ. J. Inorg. Chem.* **28,** 909 (1983/84).
14. U. L. SCHÄFER, *Neues Jahrb. Min. Monatsh.*, 75 (1980).
15. P. D. THOMPSON AND D. A. KESZLER, *Chem. Mater.* **1,** 292 (1989).
16. K. YVON, W. JEITSCHKO, AND E. PARTHE, *J. Appl. Crystallogr.* **10,** 73 (1977).
17. "TEXSAN," Molecular Structure Corp., The Woodlands, TX (1989).
18. D. STUART AND N. WALKER, *Acta Crystallogr. Sect. A* **39,** 158 (1983).
19. G. J. GILMORE, *J. Appl. Crystallogr.* **17,** 42 (1984).
20. R. D. SHANNON, *Acta Crystallogr. Sect. A* **32,** 751 (1976).
21. I. D. BROWN in "Structure and Bonding in Crystals" (M. O'Keeffe and A. Navrotsky, Eds.), Vol. II, p. 1, Academic Press, New York (1981).
22. W. C. STEELE AND J. C. DECIUS, *J. Chem. Phys.* **25,** 1184 (1956).
23. R. HOFFMANN AND W. N. LIPSCOMB, *J. Chem. Phys.* **39,** 1397 (1963).
24. C. CHEN, Y. WU, A. JIANG, B. WE, G. YOU, R. LI, AND S. LIN, *J. Opt. Soc. Am. B* **28,** 235 (1985).
25. An exception to this trend has been reported for $K_6Si_2O_7$ where $Si–O_{bridge}$ = 1.675 Å. M. JANSEN, *Z. Kristallogr.* **160,** 127 (1982).

26. B. W. McClelland, L. Hedberg, K. Hedberg, and K. Hagen, *J. Am. Chem. Soc.* **105,** 3789 (1983).
27. C. Chen, Y. Wu, A. Jiang, B. We, G. You, R. Li, and S. Lin, *J. Opt. Soc. Am. B* **28,** 235 (1985).
28. C. Chen, B. Wu, A. Jiang, and G. You, *Sci. Sin. Ser. B* **28,** 235 (1985).
29. D. Eimerl, L. Davis, S. Velsko, E. K. Graham, and A. Zalkin, *J. Appl. Phys.* **62,** 1968 (1987).